

# Torque magnetometry studies of metamagnetic transitions in single-crystal $\text{HoNi}_2\text{B}_2\text{C}$ and $\text{ErNi}_2\text{B}_2\text{C}$ at $T \approx 1.9$ K

D. G. Naugle,<sup>1,\*</sup> B. I. Belevtsev,<sup>2,†</sup> K. D. D. Rathnayaka,<sup>1</sup> S. A. Adegbenro,<sup>1</sup> P. C. Canfield,<sup>3</sup> and S.-I. Lee<sup>4</sup>

<sup>1</sup>Physics Department, Texas A&M University, TX 77843, USA

<sup>2</sup>B. Verkin Institute for Low Temperature Physics and Engineering, National Academy of Sciences, pr. Lenina 47, Kharkov 61103, Ukraine

<sup>3</sup>Ames Laboratory and Iowa State University, Ames, IA 50011, USA

<sup>4</sup>National Creative Research Center for Superconductivity and Department of Physics, Pohang University of Science and Technology, Pohang 790-784, Republic of Korea

The metamagnetic transitions in single-crystal rare-earth nickel borocarbide  $\text{HoNi}_2\text{B}_2\text{C}$  and  $\text{ErNi}_2\text{B}_2\text{C}$  have been studied at 1.9 K with a Quantum Design torque magnetometer. The critical fields of the transitions depend crucially on the angle between applied field and the easy axis [110] for  $\text{HoNi}_2\text{B}_2\text{C}$  and [100] for  $\text{ErNi}_2\text{B}_2\text{C}$ . Torque measurements have been made while changing angular direction of the magnetic field (parallel to basal tetragonal  $ab$ -planes) in a wide angular range (more than two quadrants). The results are used not only to check and refine the angular diagram for metamagnetic transitions in these compounds, but also to find new features of the metamagnetic states. Among new results for the Ho borocarbide are the influence of a multidomain antiferromagnetic state, and “frustrated” behavior of the magnetic system for field directions close to the hard axis [100]. Torque measurements of the Er borocarbide clearly show that the sequence of metamagnetic transitions with increasing field (and the corresponding number of metamagnetic states) depends on the angular direction of the magnetic field relative to the easy axis.

The rare-earth nickel borocarbides of the type  $\text{RNi}_2\text{B}_2\text{C}$  (where R is a rare-earth element) have attracted considerable interest in the last decade because of their unique superconducting and/or magnetic properties. In this article, a torque magnetometry study of metamagnetic transitions at low temperature ( $T \approx 1.9$  K) in single-crystal borocarbides with R = Ho and Er is presented. Magnetic states in these magnetic superconductors are determined by magnetic moments of R ions which lay in the  $ab$ -planes, aligning along easy axes, which are [110] for Ho and [100] for Er, respectively resulting in a high magnetic anisotropy for these compounds.

In zero field,  $\text{HoNi}_2\text{B}_2\text{C}$  is a superconductor (below  $T_c \approx 8.7$  K) and antiferromagnetic (AFM) (below the Néel temperature,  $T_N \approx 5.5$  K). For  $T \lesssim 4$  K, with increasing magnetic field  $H$  (perpendicular to the tetragonal  $c$ -axis), the sequence of transitions from antiferromagnetic ( $\uparrow\downarrow$ ) to ferrimagnetic ( $\uparrow\uparrow\downarrow$ ), non-collinear ( $\uparrow\uparrow\rightarrow$ ) and ferromagnetic-like ( $\uparrow\uparrow$ ) states takes place at critical fields  $H_{m1}$ ,  $H_{m2}$  and  $H_{m3}$ , respectively<sup>1</sup>. Neutron diffraction studies show that these magnetic states are  $c$ -axis modulated except for the non-collinear phase which is  $a$ -axis modulated<sup>2,3</sup>.

In  $\text{ErNi}_2\text{B}_2\text{C}$ , superconductivity and antiferromagnetism coexists as well ( $T_c \approx 11$  K and  $T_N \approx 6$  K). Below  $T_N$  the magnetic phases are spin-density wave (SDW) states with magnetic wave vector  $\mathbf{Q} = f\mathbf{a}^*$  (or  $\mathbf{b}^*$ , where  $\mathbf{a}^*$  and  $\mathbf{b}^*$  are reciprocal lattice vectors)<sup>4</sup>. It was found that  $f \approx 0.55$  for the AFM state. Below  $T_{WF} \approx 2.5$  K a transition to a weak-ferromagnetic (or, actually, ferrimagnetic) state takes place, in which a ferromagnetic moment (about  $0.33 \mu_B$  per Er ion) appears. With increasing field (applied in the  $ab$  plane) several metamagnetic transitions occur in this compound. Generally, the ferro-

magnetic component increases at each transition reaching the maximum value (about  $8 \mu_B/\text{Er}$ ) at the final transition to a saturated paramagnetic (or ferromagnetic-like) state at  $H \gtrsim 2$  T. The resulting metamagnetic states (except the ferromagnetic-like state) remain SDW, only the scalar  $f$  of the wave vector  $\mathbf{Q} = f\mathbf{a}^*$  changes slightly, but quite distinctly, at these transitions. The only longitudinal magnetization study of these transitions<sup>5</sup> revealed three metamagnetic transitions (and correspondingly three SDW magnetic structures) with increasing field in this compound, independent of the angle between  $H$  and the easy axis. Subsequent neutron diffraction studies<sup>4</sup> have shown, however, that for  $H \parallel [010]$  four SDW magnetic structures can be distinguished for different field ranges; whereas, only three SDW phases are seen for  $H \parallel [110]$  ([010] and [110] are the easy and hard axes, respectively).

The critical fields of metamagnetic transitions depend strongly on the angle  $\theta$  between  $H$  and the nearest easy axis (or on the angle  $\phi$  between  $H$  and the nearest hard axis) for both borocarbides<sup>1,5</sup>. In this study, a PPMS Model 550 Torque Magnetometer (Quantum Design) was used to study this dependence. It measures the torque  $\vec{\tau} = \mathbf{M} \times \mathbf{H}$ , so that  $\tau = MH \sin(\beta)$ , where  $\beta$  is the angle between the external magnetic field and the magnetization. Small (0.05-0.15 mg) single-crystal rectangular plates of  $\text{HoNi}_2\text{B}_2\text{C}$  ( $0.4 \times 0.32 \times 0.26 \text{ mm}^3$ ) and  $\text{ErNi}_2\text{B}_2\text{C}$  ( $0.37 \times 0.32 \times 0.25 \text{ mm}^3$ ) were cut and polished for this study. The torque measurements were made under changes of magnetic field for different constant angles, or changes of angular direction of the magnetic field for different constant magnetic fields.

An example of the magnetic-field dependence for  $\text{HoNi}_2\text{B}_2\text{C}$  is shown in Fig. 1, where transitions manifest themselves as sharp changes of the torque at crit-

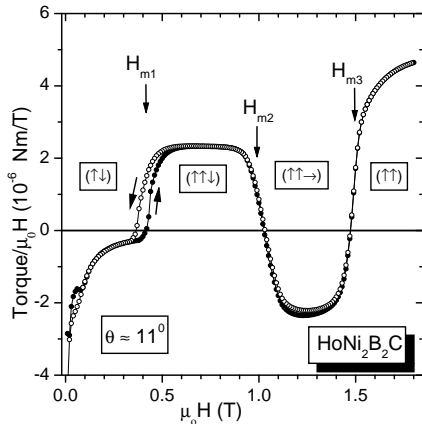


FIG. 1: Field dependence  $\tau(H)/H$  in a  $\text{HoNi}_2\text{B}_2\text{C}$  sample, recorded for increasing and decreasing magnetic field (at  $\theta \approx 11^\circ$ ). Positions of the critical transition fields  $H_{m1}$ ,  $H_{m2}$  and  $H_{m3}$  are shown by arrows. The symbols  $(\uparrow\downarrow)$ ,  $(\uparrow\uparrow\downarrow)$ ,  $(\uparrow\uparrow\rightarrow)$  and  $(\uparrow\uparrow)$  show areas of different magnetic phases.

ical fields. The angular phase diagram for  $\text{HoNi}_2\text{B}_2\text{C}$  based on these torque measurements is found to correspond generally to known experiment<sup>1</sup> and theoretical models<sup>6,7</sup>. But important new features of these metamagnetic states were found and other features made clearer as indicated below under items A, B, and C:

**(A)** According to Ref. 1, for small deviations of the magnetic field from a  $\langle 110 \rangle$  axis ( $-6^\circ \leq \theta \leq 6^\circ$ ), the  $(\uparrow\downarrow)$ – $(\uparrow\uparrow\downarrow)$ – $(\uparrow\uparrow)$  sequence of transitions takes place. In this sequence, the transition to the non-collinear  $(\uparrow\uparrow\rightarrow)$  phase is omitted. This is in disagreement with theory<sup>7</sup>, which supposes that this sequence of transitions is possible at  $\theta = 0$  only. Analysis of the magnetic-field dependences of the torque for different angles, including angles close to  $\theta = 0$ , leads to the conclusion that the angular range for this sequence of metamagnetic transitions is far less ( $-1^\circ \leq \theta \leq 1^\circ$ ) than that indicated in Ref. 1.

**(B)** The magnetization of the antiferromagnetic  $(\uparrow\downarrow)$  phase must be equal to zero, and the same should be expected for the torque (for  $H < H_{m1}$ ). It is found, however, that the magnitude  $\tau(H)/H$  is non-zero below  $H_{m1}$ . Moreover, the  $\tau(H)/H$  curves also show an appreciable field dependence with hysteretic behavior in the low-field region  $\mu_0 H < 0.1$  T (Fig. 1). This type of  $\tau(H)/H$  dependence is found for the entire angular region studied. The non-zero absolute value of  $\tau(H)/H = M \sin(\beta)$  implies that  $M \neq 0$  as well. This is possible for the AFM state if a multidomain AFM structure exists. This may result from availability of four (or at least two) equivalent easy  $\langle 110 \rangle$  directions in  $\text{HoNi}_2\text{B}_2\text{C}$ . Then, on cooling below the Néel temperature, domains can easily appear. The low-temperature orthorhombic distortions in borocarbides<sup>8</sup> could facilitate this process. When multidomain (or at least two-domain) AFM structures exist, the magnetic moments of the domains may not be completely compensated, and the torque can be non-zero. It

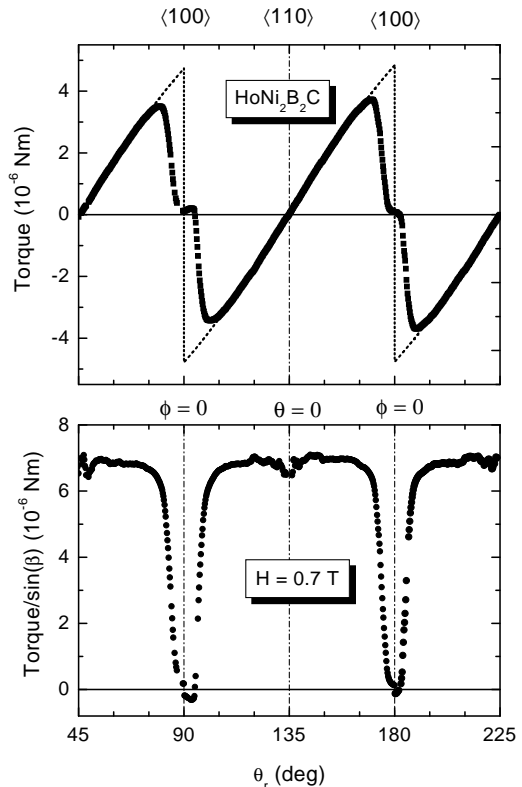


FIG. 2: Angular dependences of the torque (upper panel) and  $\tau/\sin(\beta)$  (bottom panel) at the field  $\mu_0 H = 0.7$  T in  $\text{HoNi}_2\text{B}_2\text{C}$ . The angle  $\theta_r$  represents the angular position of the rotator. The positions of the easy  $\langle 110 \rangle$  and hard  $\langle 100 \rangle$  axes together with the corresponding positions of  $\theta = 0$  and  $\phi = 0$ , are shown. The dashed line indicates the expected dependence of the torque if the transition near  $\phi = 0$  from one orientation of the ferrimagnetic state  $(\uparrow\uparrow\downarrow)$  to another  $(\rightarrow\rightarrow\leftarrow)$  were sharp.

should be noted that the torque hysteresis in the AFM phase takes place in the superconducting state. In this case, the non-zero torque and the hysteresis in the low-field range (Fig. 1) may also be related to trapped flux generated on passing through the critical field.

**(C)** The angular behavior of  $H_{m2}$  for the angles close to the hard axis  $\langle 100 \rangle$  ( $-6^\circ \leq \phi \leq 6^\circ$ ) does not follow the theoretical relation  $H_{m2}(\phi) = H_{m2}(0)/\cos(\phi)$ <sup>6,7</sup>, so that the  $H_{m2}$  values in this region are smaller than predicted. Also, in this angular range the first  $(\uparrow\downarrow)$ – $(\uparrow\uparrow\downarrow)$  and second  $(\uparrow\uparrow\downarrow)$ – $(\uparrow\uparrow\rightarrow)$  metamagnetic transitions almost merge together. This means that the width of the field range, where the ferrimagnetic  $(\uparrow\uparrow\downarrow)$  phase exists, is reduced substantially for small  $\phi$ . This "frustrated" behavior of the magnetic system shows itself in the angular torque dependences as well. In Fig. 2, the angular dependences of the torque and  $\tau/\sin(\beta)$  for  $\mu_0 H = 0.7$  T is presented. At this field only the ferrimagnetic  $(\uparrow\uparrow\downarrow)$  phase should exist for any angle<sup>1</sup>, hence the relation  $\beta = \theta$  is expected. Since  $\sin(\beta)$  changes sign on crossing the angle  $\phi = 0$  (due to reorientation of Ho moments relative to the near-

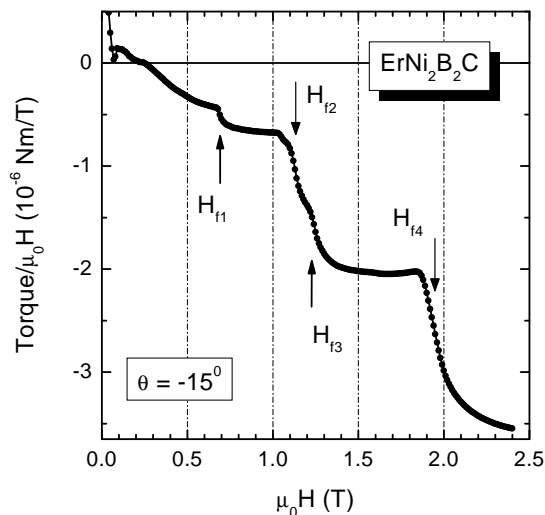


FIG. 3: Field dependence  $\tau(H)/H$  in  $\text{ErNi}_2\text{B}_2\text{C}$  sample, recorded for increasing magnetic field (at  $\theta \approx -15^\circ$ ). Positions of the critical transition fields  $H_{f1}$ ,  $H_{f2}$ ,  $H_{f3}$  and  $H_{f4}$  are shown by arrows.

est easy axis), the torque should change sign as well (Fig. 2). But  $\tau(\phi)$  behavior in the angular region close to  $\phi = 0$  does not correspond to expected behavior (shown by the dashed line) for the case  $\beta = \theta$ . It can be seen that  $\tau/\sin(\beta)$  which should be equal to the net magnetization at finite  $\beta$  goes to zero when approaching  $\phi = 0$ . Outside this region,  $\tau/\sin(\beta)$  is approximately constant as expected for the ( $\uparrow\downarrow$ ) phase. If  $\beta \neq 0$ , this would suggest that the magnetization tends to zero when the magnetic field direction approaches  $\phi = 0$ . Another possibility is that  $\sin(\beta)$  goes to zero as the field direction crosses the angle  $\phi = 0$ . In this case the magnetization at  $\phi = 0$  can be non zero, but the magnetization should be directed along the hard axis  $\langle 100 \rangle$ . Longitudinal measurements of  $\mathbf{M}$  support the latter<sup>1</sup>. This type of the torque behavior near  $\phi = 0$  was also found for higher fields where the non-collinear phase exists. The large width of the frustration region illustrated in Fig. 2, may be due to inhomogeneity induced by strain, defects or demagnetization effects. Further discussion will be presented in an extended paper.

Preliminary results for  $\text{ErNi}_2\text{B}_2\text{C}$  are shown in Figs. 3, 4. Typical  $H$  dependence of the torque for angles not far from an easy axis is shown in Fig. 3. The torque mag-

nitude increases with  $H$  and its behavior shows clearly four metamagnetic transitions, indicated by arrows. The transition fields  $H_{f1}(\theta)$  and  $H_{f2}(\theta)$  are found to be proportional to  $1/\cos(\theta)$  in agreement with results of longitudinal magnetization measurements<sup>5</sup>. On the other hand, that study<sup>5</sup> revealed clearly only one transition in the range 1.1–1.4 T; whereas, the results here show two distinct transitions (Figs. 3, 4). For angles close enough to the hard  $\langle 110 \rangle$  axis ( $-15^\circ \lesssim \phi \lesssim 15^\circ$ ) only one transition is seen in this field range (Fig. 4). The angular range in which only one transition takes place in this field range

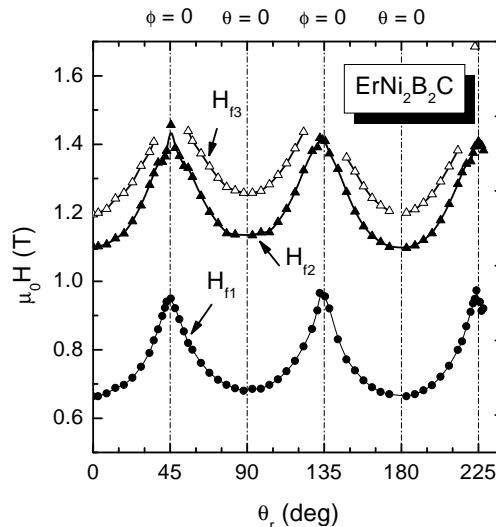


FIG. 4: The angular phase diagram of metamagnetic states in  $\text{ErNi}_2\text{B}_2\text{C}$  at  $T = 1.9$  K, obtained in this study. Results for measurements with increasing field are shown. The angle  $\theta_r$  is the modified angle on the sample rotator. The angles  $\theta_r = 0^\circ$ ,  $90^\circ$  and  $180^\circ$  correspond to different  $\langle 100 \rangle$  easy axes. The hard axes  $\langle 110 \rangle$  are shifted by  $45^\circ$ . Positions of the transition fields  $H_{f1}$ ,  $H_{f2}$  and  $H_{f3}$  are shown by arrows.

is thus determined. These results are consistent with the neutron diffraction study<sup>4</sup> for angles  $\theta = 0$  and  $\theta = 45^\circ$  (or  $\phi = 0$ ). Results of the torque study below the first transition field and for higher fields where the transitions to the paramagnetic state take place will be considered elsewhere.

This research was supported by the Robert A Welch Foundation (A-0514), NSF (DMR-0103455, DMR-0422949, DMR-0315476) and CRDF (UPI-2566-KH-03).

\* Electronic address: naugle@physics.tamu.edu

† Electronic address: belevtsev@ilt.kharkov.ua

<sup>1</sup> P. C. Canfield et al., Phys. Rev. B **55**, 970 (1997).

<sup>2</sup> A. J. Campbell et al. Phys. Rev. B **61**, 5872 (2000).

<sup>3</sup> C. Detlefs et al., Phys. Rev. B **61**, R14916 (2000).

<sup>4</sup> A. Jensen et al., Phys. Rev. B **69**, 104527 (2004).

<sup>5</sup> P. C. Canfield and S. L. Bud'ko, J. Alloys Compd. **262**, 169

(1997).

<sup>6</sup> V. A. Kalatsky and V. L. Pokrovsky, Phys. Rev. B **57**, 5485 (1998).

<sup>7</sup> A. Amici and P. Thalmeier, Phys. Rev. B **57**, 10684 (1998).

<sup>8</sup> A. Kreyssig et al., J. Appl. Phys. **85**, 6058 (1999).